Supporting Information

Construction of a sequentially responsive nanocarrier for chemotherapy and cascade amplified NIR photodynamic therapy

Tao Yan, Linlin Ren, Fengyan Li, Feng Tian, Chengfang Jiang, Qi Wang, Xinyue Song* and Shusheng Zhang*

Shandong Provincial Key Laboratory of Detection Technology for Tumor Markers, College of Chemistry and Chemical Engineering, Linyi University, Linyi 276005, P. R. China.

Corresponding author email: songxinyue428@163.com; shushzhang@126.com

Contents

1. Materials 2
2. Experimental Apparatus 2
3. Preparation of the upconversion nanotheranostic agent 3
    3.1 Preparation of UCNPs 3
    3.2 Preparation of mesoporous silica coated UCNPs (UCNPs@$mSiO_2$) 4
    3.3 Preparation of photodynamic nanotheranostic agent (UCNPs@$mSiO_2$/MB) 5
    3.4 Preparation of UCNPs@$mSiO_2$/MB@PAH 7
    3.5 DNA sequence 8
    3.6 Construction of DOX molecules loaded DNA duplex 8
    3.7 Scheme of the DNA nanoshell/DOX 9
    3.8 Design of the nanotheranostic agent UCNPs@$mSiO_2$/MB@PAH@DNA nanoshell/DOX 9
    3.9 Stability and hemocompatibility of the prepared nanomaterials 10
    3.10 Fluorescence calibration curve of DOX molecules 11
4. In vitro performance evaluation of the prepared nanotheranostic agent 12
    4.1 ATP and GSH induced the release of loaded DOX molecules 12
    4.2 Detection of the produced ROSs in aqueous solution 14
5. Cell experiment 15
    5.1 Cell culture 15
    5.2 Stability and biocompatibility of the prepared nanotheranostic agent 16
    5.3 Cellular uptake and localization of the prepared nanotheranostic agent 17
    5.4 Intracellular DOX release 18
    5.5 In vitro ROSs generation 19
    5.6 Cell apoptosis assay in living cells 20
6. Animal experiment 21
    6.1 Obtain the tumor-bearing model 21
    6.2 In vivo biodistribution and metabolism of the prepared nanotheranostic agent 22
    6.3 In vivo therapeutic efficacy assay 23
Reference 24

1. Materials

Materials for preparation of upconversion nanoparticles including rare earth oxides (purities large than 99.99%), sodium fluoride (NaF), 1-octadecene (ODE) and oleic acid (OA) were purchased from the Aladdin Reagent, Ltd. (Shanghai, China). The Sinopharm Chemical Reagent Co., Ltd. (Shanghai, China) provided the rest chemical reagents of anlytical grade. All sample solution was prepared by purified water from an OKP purification system. The animal experiments were supervised under the Animal Care and Use Committee of Linyi University.

2. Experimental Apparatus

The size and morphology of the prepared UCNPs were observed with the transmission electron microscope (TEM, model: JEM-2010, JEOL) while their crystal structure was obtained with the X-ray powder diffractometer. EDS 2D mapping analysis was achieved on STEM (mode: FEI TalosF200x). An external 980 continuous-wave laser was used to provide the excitation light for the prepared UCNPs and then their fluorescence information was recorded with the fluorescence spectrophotometer (mode: F-4600, Hitachi). Fluorescence lifetime measurements were performed with the near infrared fluorescence and phosphorescence spectrometer (FLS 980-STM, Edinburgh Instruments Ltd., Livingston, United Kingdom). Electron spin resonance analysis was used to observe the generation of reactive oxygen species. The characteristic UV absorption peaks and ζ potential of the prepared upconversion nanotheranostic agents were analyzed with the Uv-Vis spectrophotometer (model: Cary 60, Agilent) and the Zeta-size nano instrument (Zen 3600, Malvern Instruments Ltd.), respectively. The fluorescent information in the living cells was obtained with the Leica TCS SP5 confocal lasers scanning microscope. The cytotoxicity and hemocompatibility of the prepared nanomaterials were evaluated by the corresponding assay kits assisted with the Microplate Reader (Thermo Scientific Multi-skan Mk3). The cellular apoptosis experiment was achieved on the Flow Cytometry (Beckman Coulter, Inc.). The IVIS Lumina Series III was used to study the *in vivo* biodistribution and metabolism of the prepared nanotheranostic agent.

3. Preparation of the upconversion nanotheranostic agent

3.1 Preparation of UCNPs

UCNPs with three separate luminescence peaks were obtained with the structure of $NaYF_4$@$NaYF_4$,Yb:Tm@$NaYF_4$,Yb:Er@$NaYF_4$ and the adjacent two luminescence layers doped with Tm^{3+} and Er^{3+}, respectively, was used to increase the luminescence efficiency. The multi-color UCNPs were prepared via the seed-mediated layer-by-layer growth method in this experiment. Firstly, the Yttrium oleate ($Y(oleate)_3$) was obtained according to the followed procedure. Yttrium oxide Y_2O_3 (5.0 mmol) were dissolved in 30 mL of concentrated hydrochloric acid (HCl), reacted at 60°C for overnight and evaporated to acquire the solid YCl_3. The obtained YCl_3 was subsequently mixed with 20 mmol sodium oleate, then reacted in the solvent consisting of ethanol, ultrapure water and hexane with volume ratio of 4:3:7. The Yttrium oleate ($Y(oleate)_3$) was obtained via refluxing at 70°C for 6h, washed with ultrapure water by the separatory funnel and evaporated to remove the hexane.[1] The lanthanide oleate complex ($Ln(oleate)_3$) were obtained in the same way and the molar ratio was optimized to be Y:Yb:Tm=59.5:40:0.5 and Y:Yb:Er=80:18:2, respectively. Then, 20 mmol NaF and 0.5 mmol $Y(oleate)_3$ was added into 20 mL OA/ODE mixing solution (*V*:*V*=1:1), the mixture solution was heated to 110°C and reacted for 60 min under the protection of argon (Ar), then further heated to 320°C and reacted for another 90 min to form $NaYF_4$ core. Then, 0.8 mmol $Ln(oleate)_3$ (Y:Yb:Tm=59.5:40:0.5) was injected into the above reaction solution and reaction at 320°C for another 20 min to form the first luminescent shell on the surface of $NaYF_4$ core. And then, the same amount of $Ln(oleate)_3$ (Y:Yb:Er=80:18:2) was injected and reacted for 20 min to grow the second luminescent shell. After that, 0.6 mmol $Y(oleate)_3$ was injected into the above mixture solution and reacted for another 20 min to grow the outer protection layer. Finally, the reaction mixture was cooled to the room temperature. The prepared multi-color UCNPs was

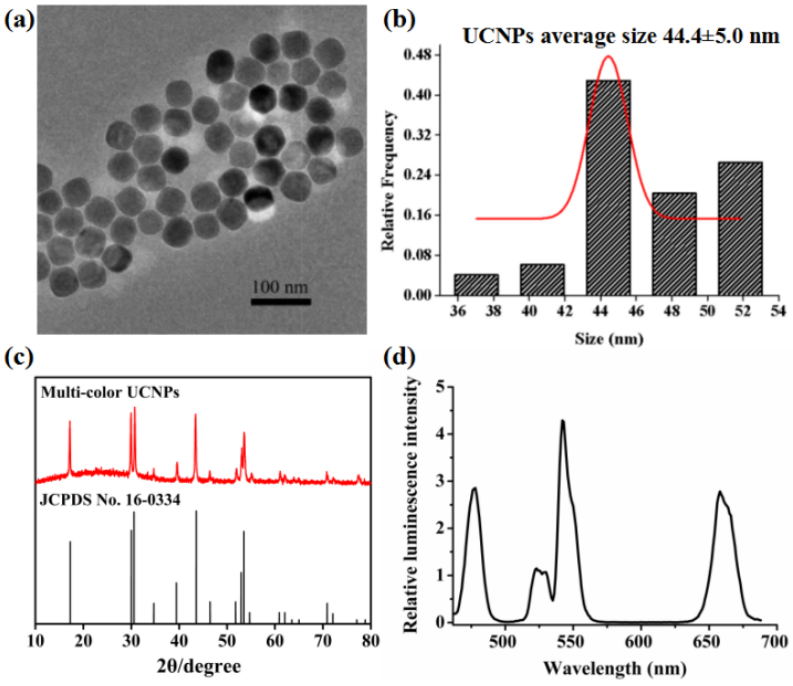

precipitated by two-fold volume of ethanol, centrifugally collected, washed with hexane/ethanol (*V:V*=1:6) for several times and dispersed in hexane for further use.

Figure S1: (a) transmission electron microscope (TEM) image; (b) size distribution; (c) X-ray diffraction (XRD) images; (d) relative luminescence intensity of the prepared multi-color UCNPs.

3.2 Preparation of mesoporous silica coated UCNPs (UCNPs@$mSiO_2$)

Usually, there were two commonly-used methods to synthesize the UCNPs@$mSiO_2$. The first method is to directly coat $mSiO_2$ layers on the surface of UCNPs in one step while the second method is to coat $mSiO_2$ layers on the surface of dense silica coated UCNPs (UCNPs@$dSiO_2$) to synthesize the UCNPs@$dSiO_2$@$mSiO_2$ with the structure of core@shell@shell.[2] Shi et al. group reported the direct fabrication of $mSiO_2$ layers with thickness of around 20-100 nm on the hydrophobic surface of UCNPs using temperature-controlled ultrasonication treatment which needed to finely control the reaction parameters such as the added amount and rate of the silica precursor, pH of the reaction mixture and added sequence of reagent.[3] Here we developed a novel and feasible method to prepare UCNPs@$mSiO_2$ with thin thickness. Firstly, hydrophilic bared UCNPs was prepared by the acid-treatment. Oleic acid protected UCNPs (20 mg) was centrifugated, then dispersed in 20 mL of acidic ethanol solution (pH=1) and ultrasonicated for 1 h to remove the surface oleate ligand. The obtained bared UCNPs were collected after washed with ethanol and dispersed in ultrapure water for further use. Then, the surfactant, hexadecyltrimethylammonium chloride (CTAC, 1.0 g) and organic base, triethanolamine (0.01 g), were mixed into 10 mL of ultrapure water and stirred for 90 min. After that, 20 mg bared UCNPs was added dropwise and reacted for another 90 min. Subsequently, the silica precursor, tetraethyl orthosilicate (TEOS, 80 μL) was slowly added and reacted at 80^{o}C for 90 min to grow a homogeneous silica layer on the surface of UCNPs. To obtain the mesoporous silica, the surfactant CTAC was removed with the developed substitution method. Briefly, the above silica layer coated UCNPs was collected by centrifugation, added into 1 wt% solution of sodium chloride (NaCl) in ethanol (30 mL) and stirred for overnight. Then, nanoparticles was obtained after centrifugation and washed with ethanol for twice. The above substitution process in ethanol solution containing 1.0 wt % of NaCl was repeated twice and each process lasted for 3 h for the complete substitution of surfactant CTAC. Finally, the obtained UCNPs@$mSiO_2$ was dispersed in 5.0 mL of ultrapure water for further use.

The prepared UCNPs@$mSiO_2$ was characterized with EDS 2D mapping analysis. As shown in Figure S2 showed that Na^+ and Y^+ ions distributed mainly in the inner UCNPs core while Si^{4+} distributed mainly in the outer shell, proving the successful preparation of the core-shell structured UCNPs@$mSiO_2$ nanoprobe.

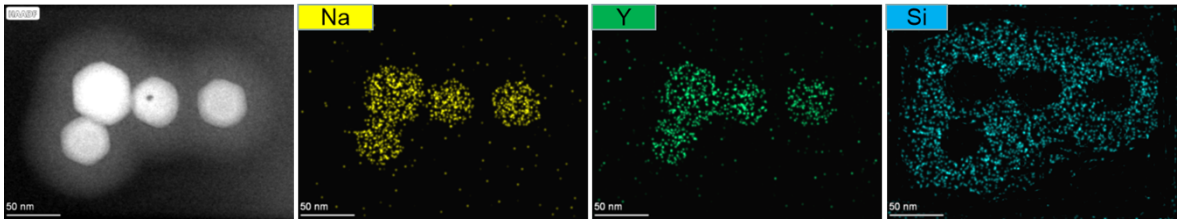

Figure S2: EDS 2D mapping of the distribution of Na^{+}, Y^{3+} and Si^{4+} in the prepared UCNPs@$mSiO_2$ nanoprobe.

3.3 Preparation of photodynamic nanotheranostic agent (UCNPs@$mSiO_2$/MB)

In this experiment, photosensitizer, methylene blue (MB), was loaded into the mesoporous silica to prepare the upconversion photodynamic nanotheranostic agent (UCNPs@$mSiO_2$/MB). Briefly, MB aqueous solution (250 μL, 1.0 mg/mL) was added into UCNPs@$mSiO_2$ aqueous solution (10 mL, 1.0 mg/mL) and then stirred for overnight at room temperature. The prepared UCNPs@$mSiO_2$/MB (1.0 mg/mL) was stored in ultrapure water after washed with water and HEPES buffer solution for several times to remove excess MB molecules.

The successful loading of MB into the prepared UCNPs@$mSiO_2$ nanoprobe was further validated by the ζ-potential analysis and Uv-Vis spectrometer analysis. The prepared UCNPs@$mSiO_2$/MB showed an increase in ζ-potential from -32.8 mv to -14.9 mv (Figure S3a) and displayed the characteristic Uv-Vis absorption peak of MB molecules (Figure S3b). In addition, the prepared UCNPs@$mSiO_2$/MB nanoprobe could keep the well distribution (Figure S3c).

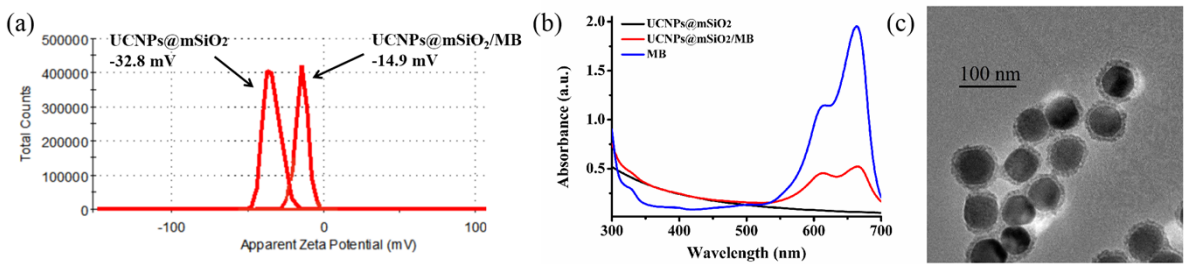

Figure S3: (a) ζ-potential analysis of UCNPs@$mSiO_2$ and UCNPs@$mSiO_2$/MB; (b) Uv-Vis of UCNPs@$mSiO_2$, UCNPs@$mSiO_2$/MB and MB molecules; (c) TEM image of UCNPs@$mSiO_2$/MB.

The energy transfer efficiency between UCNPs and MB molecules was evaluated with the luminescence lifetime assay.[4] Fluorescence lifetime measurements were performed using with the near infrared fluorescence and phosphorescence spectrometer (FLS 980-STM, Edinburgh). The decay curves were mono- to tetra- exponentially fitted using reconvolution fit analysis with following equation included in FLS-980 software. The fitting formula is:

$$R(t) = A + B_1\, e^{(-t/\tau_1)} + B_2\, e^{(-t/\tau_2)} + B_3 e^{(-t/\tau_3)} + B_4 e^{(-t/\tau_4)}$$

where t is time, A is a constant background, B_1, B_2, B_3, and B_4 are fractional intensities, τ_1, τ_2, τ_3, and τ_4 are fluorescence lifetimes. The amplitude-weighted average fluorescence lifetime $<\tau>$ is calculated from following equation:

$$<\tau>=(B_1\tau^2_1+B_2\tau^2_{2+}B_3\tau^2_{3+}B_4\tau^2_4)/(B_1\tau_1+B_2\tau_{2+}B_3\tau_{3+}B_4\tau_4)$$

The luminescence lifetimes of UCNPs@$mSiO_2$/MB and UCNPs@$mSiO_2$ at emission wavelength of 659 nm were detected to be 183.35 μs (x^2=1.140) and 269.22 μs (x^2=1.300), respectively. According to the equation $E=(1-\tau_1/\tau_2)\times100\%$, where τ_1 and τ_2 represented for the luminescence lifetime of UCNPs@$mSiO_2$/MB and UCNPs@$mSiO_2$, respectively, the calculated energy transfer efficiency between UCNPs and MB molecules was 31.90%, which was comparable to the reported energy transfer efficiency.[5]

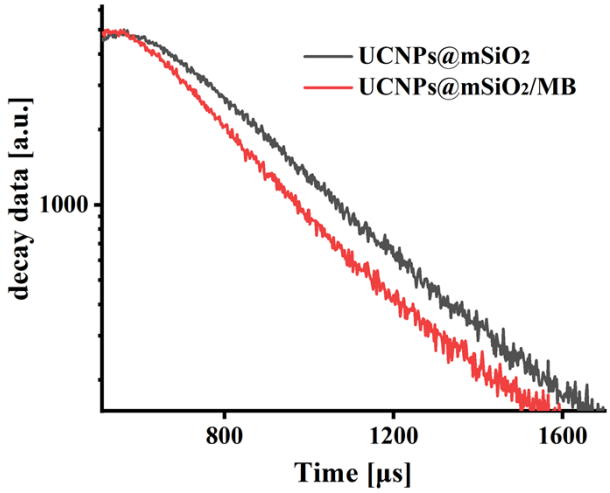

Figure S4: Fluorescence lifetime curves of the prepared UCNPs@$mSiO_2$ (blank line) and UCNPs@$mSiO_2$/MB (red line). The lifetime was measured in the emission channel of 659 nm excited by 980 nm laser.

Electron spin resonance analysis was used to directly detect the generated ROSs. Here, we chose 2,2,6,6-tetramethyl-4-piperidone (4-oxo-TEMP) as a spin trap to detect $^1O_2$.[6] As shown in Figure S5, the ESR signals of the prepared UCNPs@$mSiO_2$/MB under the excitation exhibited an obvious 1:1:1 triplet spectrum, which was the characteristic spectrum of the adduct formed between 4-oxo-TEMP and $^1O_2$ while no ESR signals were observed for UCNPs@$mSiO_2$/MB without the excitation owing to the absence of LRET between UCNPs and MB molecules.

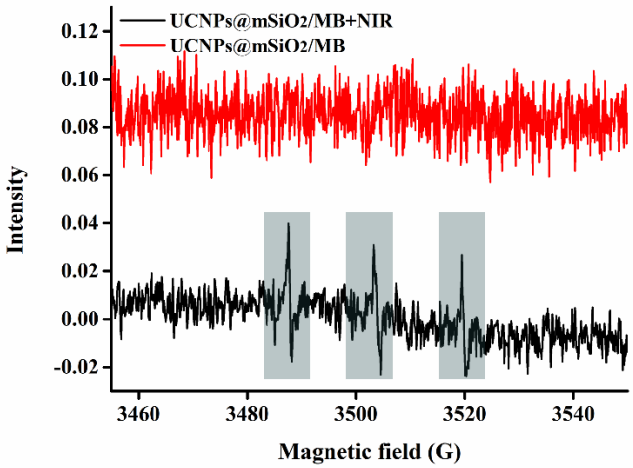

Figure S5: ESR spectra of 4-oxo-TEMP/$^1O_2$ for the prepared UCNPs@mSiO$_2$ with and without the excitation of 980 nm laser.

3.4 Preparation of UCNPs@mSiO$_2$/MB@PAH

The obtained upconversion photodynamic nanotheranostic agent, UCNPs@mSiO$_2$/MB (2.0 mg), was dispersed in 2.0 mL of PAH aqueous solution (0.6 mg/mL). After being stirred for 6.0 h, the obtained UCNPs@mSiO$_2$/MB@PAH was centrifugated, washed with ultrapure water for three time and dispersed in ultrapure water for further use.

As shown in Figure S6a, the modification of PAH would largely increase the ζ-potential of the nanoprobe from -14.9 mV to 45.4 mV owing to the protonation effect of the surface -NH$_2$ group, which was beneficial to deliver nucleic acids. As expected, PAH polymer formed a uniform protection layer on the surface of UCNPs@mSiO$_2$/MB as shown in Figure S6b.

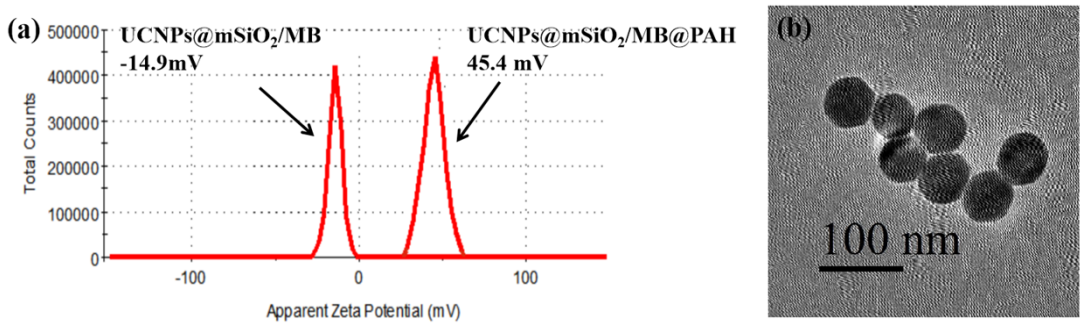

Figure S6: (a) ζ-potential analysis of UCNPs@mSiO$_2$/MB and UCNPs@mSiO$_2$/MB@PAH; (b) TEM image of UCNPs@mSiO$_2$/MB@PAH.

3.5 DNA sequence

Table S1: Special sequence of used DNA

	Sequence (5'-3')
DNA 1	gaa tcg att a/SH-SH/ccc cca gg

Non-modified DNA 1	gaa tcg att acc ccc agg
DNA 2	tcg att c**cc tgg ggg agt att gcg gag gaa ggt** ggc tat agc aca tgg gt (ATP aptamer was bold labeled and underlined)
DNA 3	acc ttc ct/SH-SH/ ttt acc cat gtg cta tag cc
Non-modified DNA 3	acc ttc ctt tta ccc atg tgc tat agc c
DNA 4	tcg att c**cc tgg ggg agt att gcg gag gaa ggt** ggc tat agc aca tgg gtg cag ttg atc ctt tgg ata ccc tgg (ATP aptamer was bold labeled and underlined, MUC1 aptamer was labeled in emerald green)

3.6 Construction of DOX molecules loaded DNA duplex

Firstly, the DNA hybrids include the hybrid (1)/(2), the hybrid DNA (2)/(3) and the hybrid DNA (1)/(4) were obtained through the annealing procedure which were verified by the PAGE gel analysis.

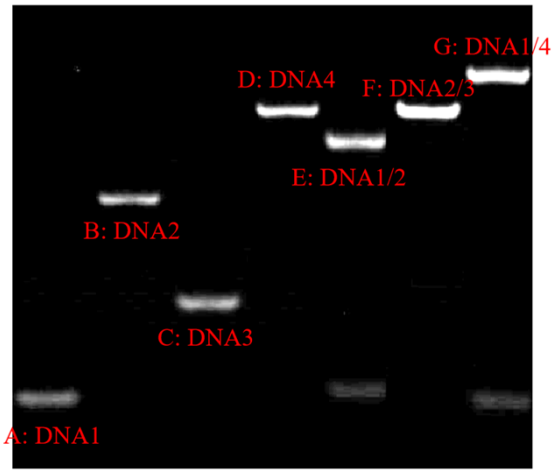

Figure S7: PAGE gel analysis of the used DNA strands in this experiment. The concentrations of DNA strands were 1.0 μM. The hybridized DNA strands include DNA hybrid (1)/(2), DNA hybrid (2)/(3) and DNA hybrid (1)/(4) were achieved in TE buffer (pH-8.0 containing 10 mM Mg^{2+}) by the annealing process.

It was reported that the fluorescence intensity of DOX molecules would be sequentially decreased due to the intermolecular förster resonance energy transfer when intercalated into DNA duplex. Besides, the decrease degree showed a good correlation with the molar ratio of DNA duplex. As shown in Figure S8, both of the optimum molar ratio of DNA hybrid (1)/(2) to DOX molecules and DNA hybrid (2)/(3) to DOX molecules was calculated to be 0.3:1. Thus, the corresponding DOX molecules was added into the DNA duplex and reacted for overnight to obtain the dsDNA/DOX in this experiment. Briefly, two DNA double strands, the hybrid (1)/(2) and the hybrid DNA (2)/(3), was obtained via the conventionally-used annealing procedure. Then, 5.0 nmol of DOX molecules were added into 10 μM of the DNA hybrid (1)/(2)

(150 μL) and DNA hybrid (2)/(3) (150 μL), respectively, and then incubated overnight to obtain the DNA hybrid (1)/(2)/DOX and DNA hybrid (2)/(3)/DOX, respectively.

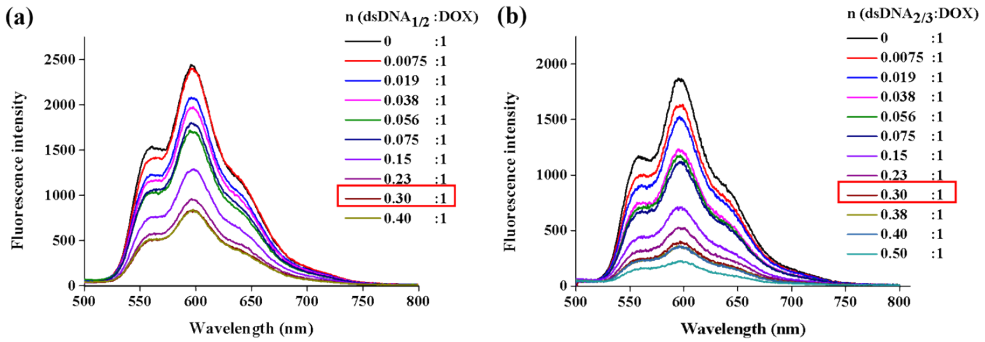

Figure S8: the fluorescence spectra of 5.3 μM DOX in the HEPES buffer (20 mM, pH-7) with increasing molar ratios of the DNA hybrid (1)/(2) (a) and the DNA hybrid (2)/(3) (b) after incubation for 6 h.

3.7 Scheme of the DNA nanoshell/DOX

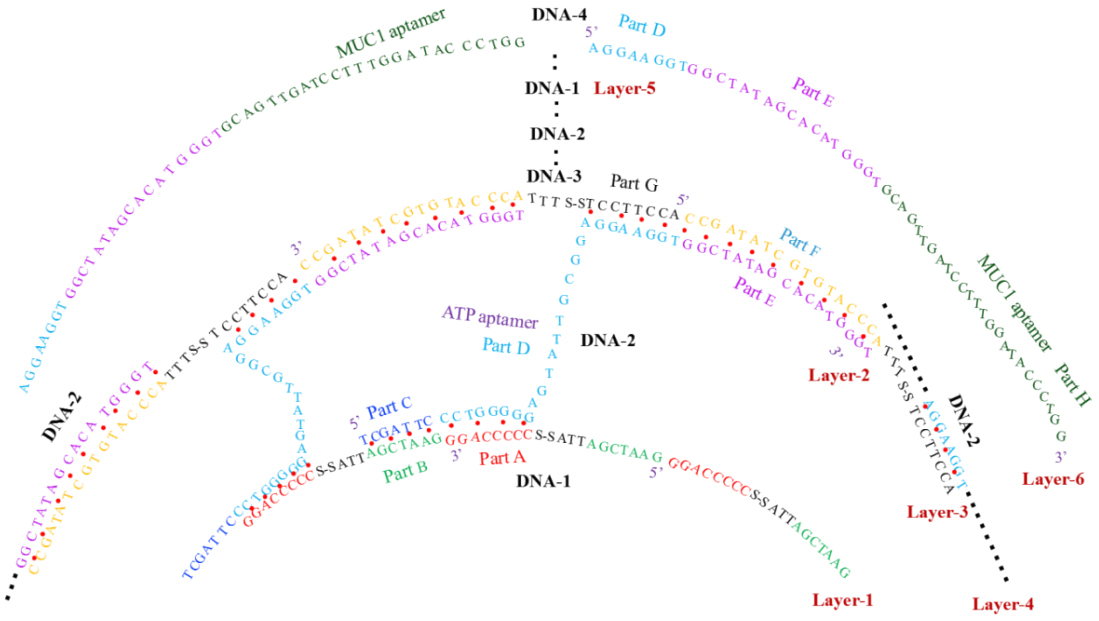

Figure S9: Scheme of the formed DNA nanoshell. The red dot represented for DOX molecules.

3.8 Design of the nanotheranostic agent UCNPs@mSiO$_2$/MB@PAH@DNA nanoshell/DOX

The final upconversion nanotheranostic agent, was obtained by the layer-by-layer self-assembly method. Briefly, UCNPs@mSiO$_2$/MB@PAH solution (2.0 mL, 1.0 mg/mL) was coated with the designed DNA nanoshell by sequential incubation in DNA hybrid (1)/(2)/DOX (100 μL, 10 μM) or DNA hybrid (2)/(3)/DOX (100 μL, 10 μM) or DNA hybrid (1)/(4)/DOX (100 μL, 10 μM) for 4 h. After each incubation, two washing steps were performed to remove the excess non-adsorbed DNA. Guided by the above procedure, the final upconversion nanotheranostic agent, UCNPs@mSiO$_2$/MB@PAH@DNA nanoshell/DOX, with concentration of 2.5 mg/mL

were obtained with six layers of DNA coating.

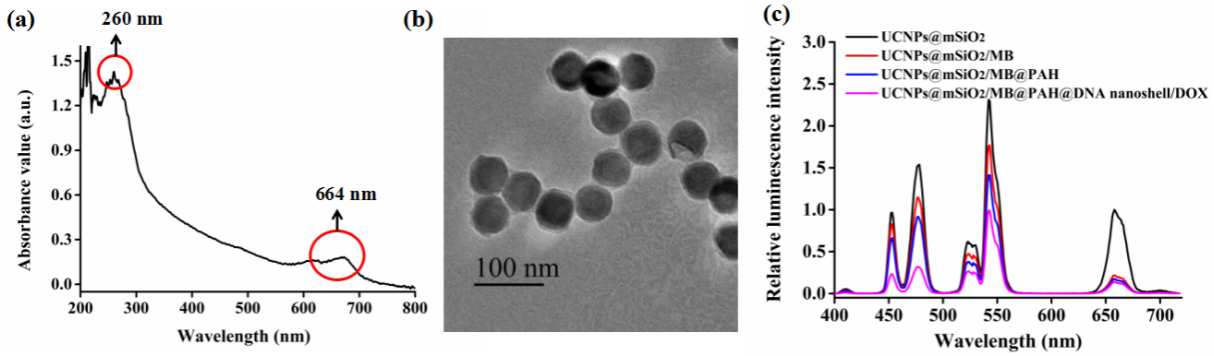

Figure S10: (a) Uv-Vis spectra of the prepared UCNPs@mSiO$_2$/MB@PAH@DNA nanoshell/DOX; (b) TEM spectra of the prepared UCNPs@mSiO$_2$/MB@PAH@DNA nanoshell/DOX; (c) relative luminescence spectra of UCNPs@mSiO$_2$, UCNPs@mSiO$_2$/MB, UCNPs@mSiO$_2$/MB@PAH and UCNPs@mSiO$_2$/MB@PAH@DNA nanoshell/DOX.

3.9 Stability and hemocompatibility of the prepared nanomaterials

To validate the stability of the prepared nanomaterials, we compared the change in their dispersibility, relative fluorescence intensity and Uv-Vis absorbance spectra within one week. As shown in Figure S11, the prepared nanoprobes still kept well dispersibility after one week. Besides, there was no obvious change in their luminescence intensity and Uv-Vis spectra.

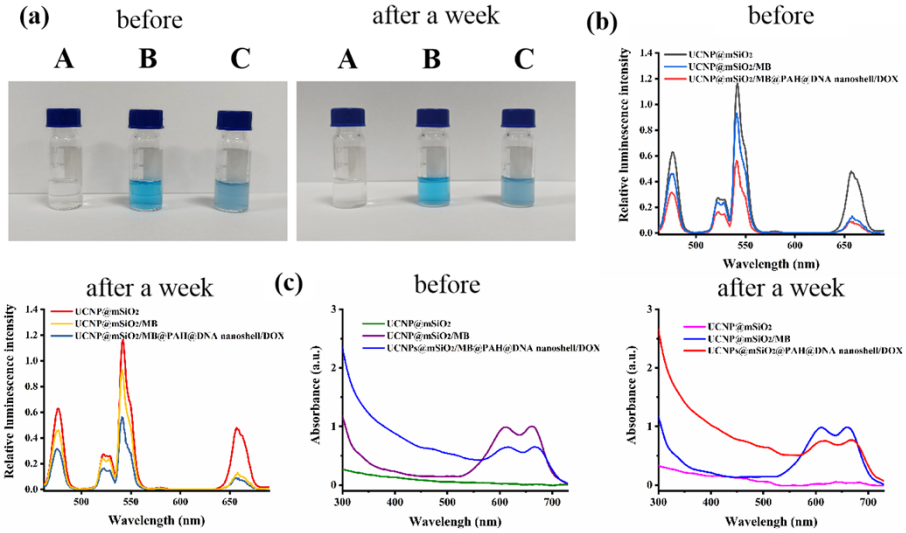

Figure S11: (a) Graphs of the prepared nanomaterials, A-C represented for the prepared UCNP@mSiO$_2$, UCNP@mSiO$_2$/MB and UCNP@mSiO$_2$/MB@PAH@DNA nanoshell/DOX, respectively; (b) Relative luminescence spectra of the nanomaterials which were newly prepared and kept for one week ; (c) Uv-Vis spectra of the nanomaterials which were newly prepared and kept for one week.

Furthermore, the hemocompatibility of the prepared nanomaterials was evaluated according to the references.[7] Briefly, red blood cells (RBCs) in 2 ml of fresh newborn bovine blood sample were separated by centrifugation at 2000 rpm for 5 min, washed three times with

physiological saline, then resuspended in saline solution. The diluted RBCs suspension was incubated with the prepared nanoprobes (0.1 mg/mL) and then kept at 37°C for 2 h to induce hemolysis. Finally, the mixture was centrifuged at 2000 rpm for 5 min, and 100 μL of the obtained supernatant was transferred to a 96-well plate where its absorbance values at 490 nm were detected using a microplate reader. Diluted RBCs suspension (0.2 mL) incubated with physiological saline (0.8 mL) and water (0.8 mL) was used as a negative or positive control, respectively. The hemolysis percent of RBCs was calculated using the following formula: hemolysis (%) = (sample absorbance-negative control absorbance) / (positive control absorbance-negative control absorbance)×100. Each experiment contained six parallel groups.

As shown in Figure S12, 0.1 mg/mL of the prepared nanomaterials displayed less than 12.3% of hemolytic activity. Thus, the designed nanotheranostic agent owned good hemocompatibility, which offered great potential for their *in vivo* biomedical applications involving intravenous administration and transport.

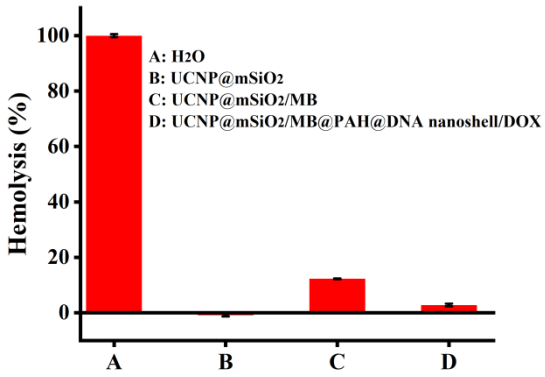

Figure S12: Percentage of hemolysis of red blood cells incubated with 0.1 mg/ml of A) H_2O, B) UCNPs@$mSiO_2$, C) UCNPs@$mSiO_2$/MB, D) UCNPs@$mSiO_2$/MB@PAH@DNA nanoshell/DOX.

3.10 Fluorescence calibration curve of DOX molecules

In order to quantify released DOX molecules, a series of DOX aqueous solution in the concentration range of 0.0001-0.002 mg/mL was analyzed by the fluorescence spectrometry. As shown in Figure S13, the obtained fluorescence calibration curve was y=989834.56x+111.91 with correlation coefficient R^2=9984.

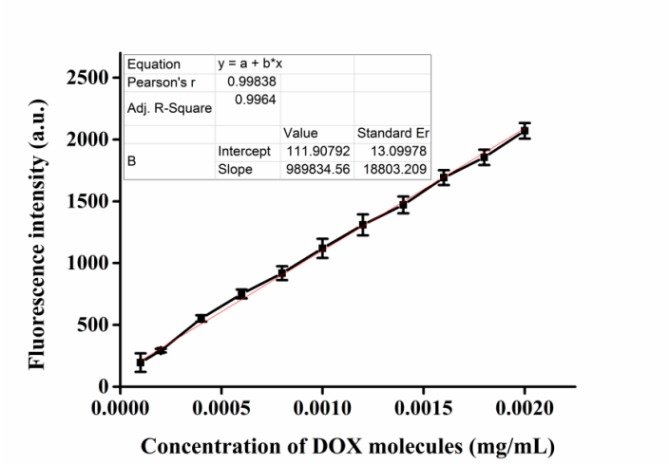

Figure S13: The fluorescence calibration curve of DOX molecule.

4. In vitro performance evaluation of the prepared nanotheranostic agent

4.1 ATP and GSH induced the release of loaded DOX molecules

The solution of the prepared nanotheranostic agent (100 μL, 2.5 mg/mL) were mixed with GSH or ATP in different concentration range. After reacting for certain time, the mixture solution was centrifugated and the supernatants was analyzed with the fluorescence spectrophotometer to record the fluorescence information of DOX molecules and calculate their release ratio.

Based on the fluorescence intensity of DOX in supernatants and the obtained calibration curve, the amount of released DOX could be obtained for evaluating the release efficiency of the designed nanotheranostic agent. As shown in Figure S14a, the released amount of DOX molecules improved with the concentration of GSH increasing from 0.3 mM to 10 mM, and the released ratio could reach to 36.3-63.2% when triggered by GSH with concentration of 2-10 mM. Contrarily, DOX molecules showed negligible release when triggered by GSH with its extracellular concentration of 2-50 μM. Considering the strong binding of ATP aptamer to ATP, the formed DNA nanoshell would be broken and then release free DOX molecules. As proved by Figure S14b, the released amount of DOX molecules improved in the concentration range of ATP from 0-15 mM and the highest release efficiency could reach to 40.80% at 15 mM of ATP. Then, we considered the cooperative release ability of the prepared nanotheranostic agent. As demonstrated in Figure S14c, the designed nanotheranostic agent showedincreased release amount and the highest release efficiency could reach to 77.5% at 10 mM GSH and ATP. Subsequently, we studied the release kinetics of the prepared nanotheranostic agent. As shown in Figure S14d, the prepared nanotheranostic agent showed a boom-like release when triggered by GSH which could be nearly finished after 5 min. Besides, the release could reach to equilibrium at 30 min when triggered by ATP (Figure S14e). The release speed could be further accelerated due to the cooperative function of ATP and GSH (Figure S14f).

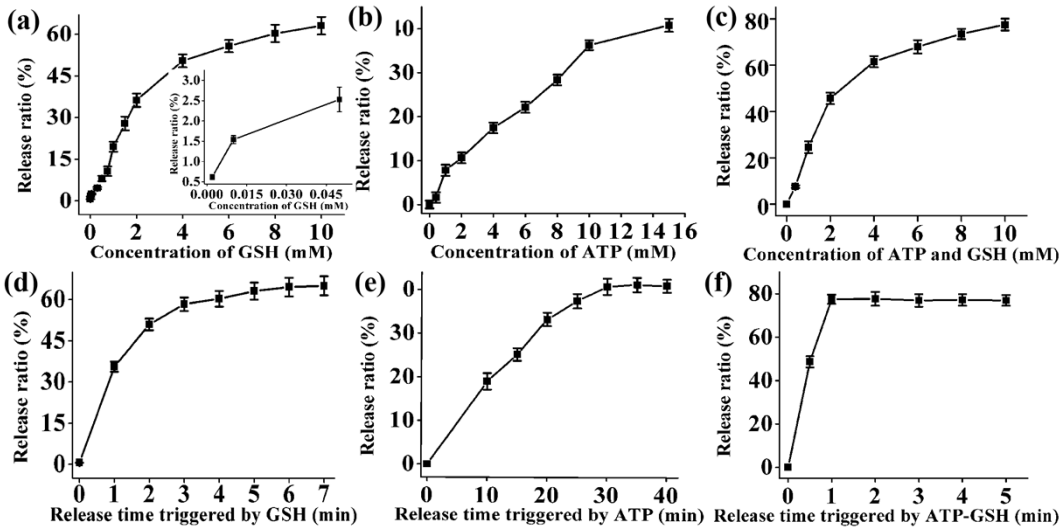

Figure S14: Release ratio of DOX molecules when the prepared nanotheranostic agent was triggered by (a) GSH; (b) ATP; (c) ATP and GSH; release kinetics of DOX molecules when the prepared nanotheranostic agent was triggered by (d) 10 mM of GSH; (e) 10 mM of ATP; (f) 10 mM of ATP and GSH.

When the molar ratio of DNA hybrid (1)/(2)/DOX to DNA hybrid (2)/(3)/DOX was set 2:1, 2:2 and 3:2, respectively, thus around six, eight and ten DNA layers formed the DNA nanoshell. As shown in Figure S15a, the release ratio of DOX molecules decreased with the increase in the number of DNA layers since the over dense of DNA nanoshell was unfavorable for the release of loaded drug molecules. Beside the number of DNA layers, the rational design of DNA strand could also achieve the controlled release of loaded drugs. A decrease in the release ratio of DOX molecules and an increase in the equilibrium time were observed for the nanotheranostic agent made of DNA strand without the modification of disulfide bond (Figure S15b-S15c).

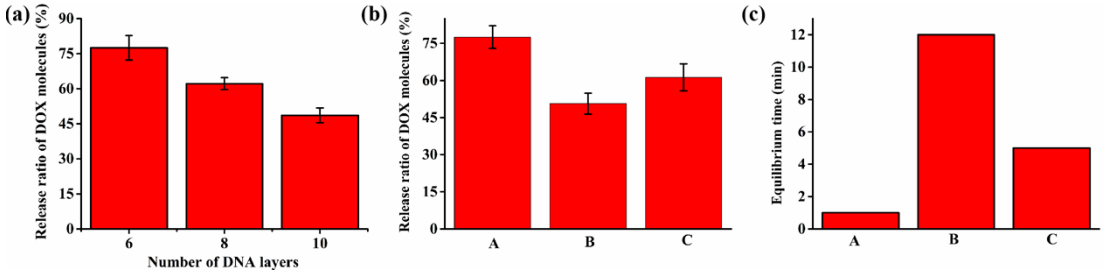

Figure S15: (a) Effects of the number of DNA layers on the release ratio of DOX molecules; (b) Effects of the DNA structure on the release ratio of DOX molecules; (c) Effects of the DNA structure on the equilibrium time of the released DOX molecules. A represented for the nanotheranostic agent prepared by DNA-1 with disulfide bond and DNA-3 with disulfide bond; B represented for the nanotheranostic agent prepared by non-modified DNA-1 and DNA-3; C represented for the nanotheranostic agent prepared by DNA-1 and non-modified DNA-3. The formed nanotheranostic agent was triggered by 10 mM of ATP and GSH for 5 min.

4.2 Detection of the produced ROSs in aqueous solution

1,3-diphenylisobenzofuran (DPBF) could irreversibly react with ROSs to cause the corresponding decrease in its Uv-Vis absorbance intensity at 410 nm.[8] Thus, DPBF was used to evaluate the generated amount of ROSs induced by the prepared nanotheranostic agent. Briefly, 1.0 mg/mL of the prepared nanotheranostic agent was mixed with 0.02 mg/mL DPBF, irradiated with 980 nm continuous-wave laser for 40 min with an interval of 5 min, and then recorded its Uv-Vis absorbance information at 410 nm. As shown in Figure S16a, the prepared nanotheranostic agent induced a negligible decrease in the Uv-Vis absorbance intensity of DPBF due to the little produced ROSs, proving the protection function of the surface DNA nanoshell could prevent the inner PSs from reacting with oxygen to produce ROSs. Once the prepared nanotheranostic agent was triggered by ATP and GSH, the outer DNA nanoshell was broken, making the loaded PSs active and then producing ROSs under the excitation of NIR laser (Figure S16b-S16d). Besides, their ability to produce ROSs was comparable to those of the previously prepared UCNPs@mSiO$_2$/MB and UCNPs@mSiO$_2$/MB@PAH nanoprobe (Figure S17). In this experiment, the formed DNA nanoshell could not only achieve the activatable chemotherapy with fast response to TME, but also be used to design the controllable and pre-protective PDT.

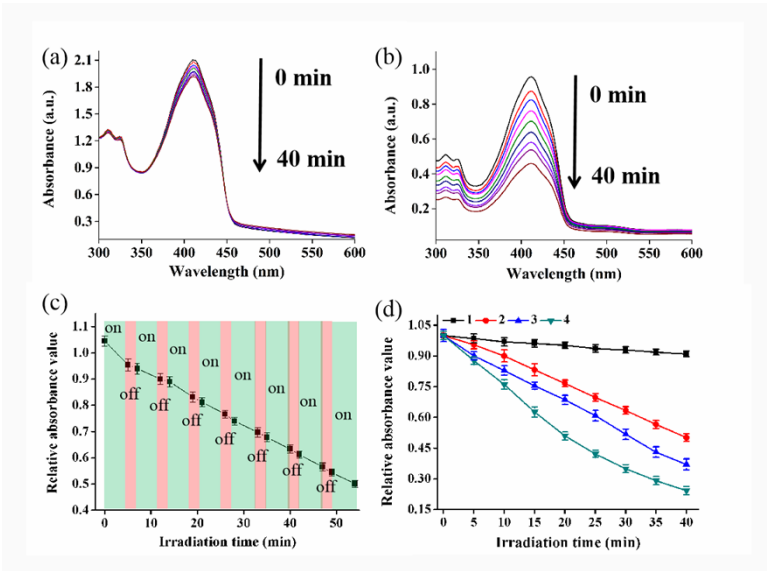

Figure S16: Absorbance value of DPBF when mixed with the prepared nanotheranostic agent and irradiated under 980 nm laser (1.5 W/cm^2) (a) before the stimulus of ATP and GSH (labeled as probe 1); (b) after the stimulus of ATP and GSH (labeled as probe 2); (c) On-off examination of ROSs production for the prepared nanotheranostic agent under the irradiation of 980 nm laser; (d) the relative absorbance value of DPBF when mixed with different nanoprobe and irradiated under 980 nm laser. The prepared UCNPs@mSiO$_2$/MB@PAH was labeled as probe 3 and the prepared UCNPs@mSiO$_2$/MB was labeled as probe 4.

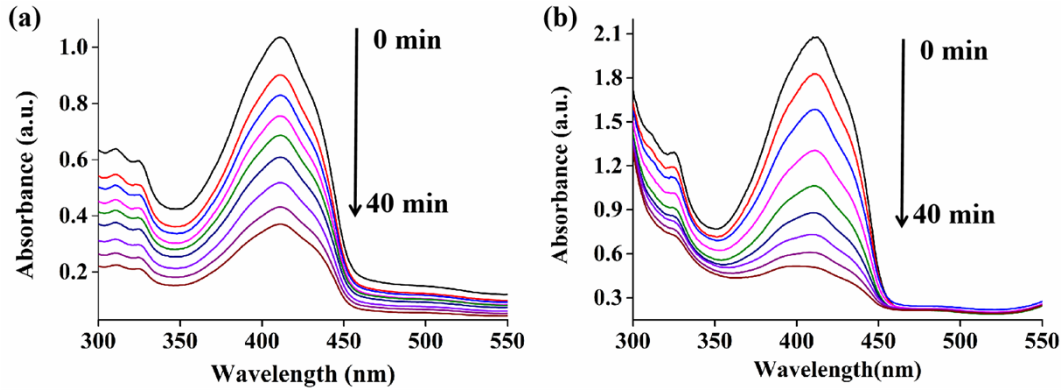

Figure S17: Absorbance value of DPBF when mixed with 1.0 mg/mL of the prepared (a) UCNPs@mSiO$_2$/MB@PAH or (b) UCNPs@mSiO$_2$/MB and then irradiated under 980 nm laser for 40 min with an interval of 5 min.

5. Cell experiment

5.1 Cell culture

The cell culture solution for A549 cancer cells chose Dulbecco's modified Eagle's medium (DMEM) including 10% heat-inactivated fetal bovine serum (FBS), penicillin (100 U/mL), and streptomycin (100 U/mL) and the cell culture environment was set at 37^{o}C, humidified air and 5% CO_2.

5.2 Stability and biocompatibility of the prepared nanotheranostic agent

The stability of the prepared nanotheranostic agent, UCNPs@mSiO$_2$/MB@PAH@DNA nanoshell/DOX was investigated by examining the DOX leakage when incubated in 10% fetal bovine serum buffer. After certain time, the release percentage of DOX molecules in the 10% fetal bovine serum buffer was detected and calculated according to the standardization curve of fluorescence intensity. As shown in Figure S18a, the release percentage of DOX molecules in the 10% fetal bovine serum buffer was less than 8.0% within 24 h.

The cell cytotoxicity of the corresponding nanotheranostic agent, UCNPs@mSiO$_2$@PAH@DNA nanoshell was evaluated according to the CCK-8 assay. Briefly, A549 cancer cells were firstly incubated in the 96-well flat-bottom microtiter plates for 12 h and then incubated with different concentrations of the prepared nanoprobe for 12 h, 24 h and 36 h, respectively. Each concentration was examined in four parallel wells. After different treatments, A549 cancer cells were stained with 10 μL of CCK-8 agent and then detected their absorbance at 450 nm with the microplate reader after 1 h. The cell viability was calculated according to the followed equation: Cell viability (%)=(Mean Absorbance $_{\text{treated wells}}$ - Mean Absorbance $_{\text{blank wells}}$) /(Mean Absorbance $_{\text{control wells}}$ - Mean Absorbance $_{\text{blank wells}}$) ×100. To study the effects of laser irradiation time on the cell viability, A549 cancer cells cultured in the 96-

well flat-bottom microtiter were incubated with 80 μg/mL of the prepared nanoprobe for 12 h and then irradiated with the 980 nm continuous-wave laser for different time. After incubated in the cell incubator for another 12 h, the treated A549 cancer cells was stained with 10 μL of CCK-8 agent for 1 h and then detected their absorbance at 450 nm to calculate the cell viability. As shown in Figure S18b, there was negligible cell death induced by the used irradiation intensity even at the irradiation time of 32 min, meanwhile the prepared nanotheranostic agent would not induce obvious cell cytotoxicity in the concentration range of 0.08-0.14 mg/mL within 36 h (Figure S18c).

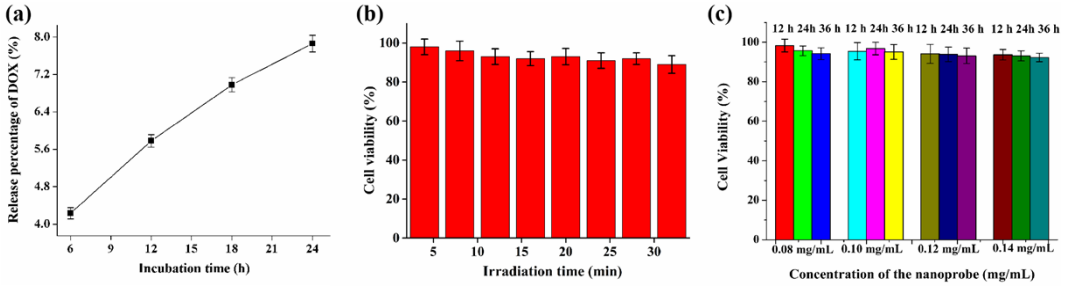

Figure S18: (a) release percentage of DOX molecules when the prepared nanotheranostic agent mixed in the 10% fetal bovine serum buffer within 24 h; (b) cell viability when treated with the control nanoprobe UCNPs@mSiO$_2$@PAH@DNA nanoshell and then irradiated with 980 nm laser with power density of 1.5 w/cm^2 for different time; (c) cell viability of A549 cancer cells when treated with different concentrations of the prepared UCNPs@mSiO$_2$@PAH@DNA nanoshell within 36 h.

5.3 Cellular uptake and localization of the prepared nanotheranostic agent

The prepared nanotheranostic agent (80 μg/mL) was added into A549 cancer cells or L132 normal cells cultured in clean glass coverslips for 2 h, 5 h and 8 h, respectively. After washed with sterile PBS buffer to remove excess probes, cells was stained with the commercial fluorescence dye, Lyso-tracker Red for another 30 min. After washed with cold PBS buffer for several times, the treated cells were observed with the two-photon laser confocal scanning microscope. The fluorescence information of the designed nanoprobe was recorded in the green channel with wavelength range of 500-570 nm under the excitation of 980 nm laser meanwhile the florescence information of the cellular lysosome was recorded in the red channel with the wavelength range of 575-635 nm under the excitation of 561 nm.

To validate its targetability, the uptake of the designed nanotheranostic agent into A549 cancer cells and L132 normal cells was further studied. As shown in Figure S19, there was obvious decreased in the uptake of the prepared nanotheranostic agent into the normal cells versus that of cancer cells owing to the targetability of MUC1 aptamer.

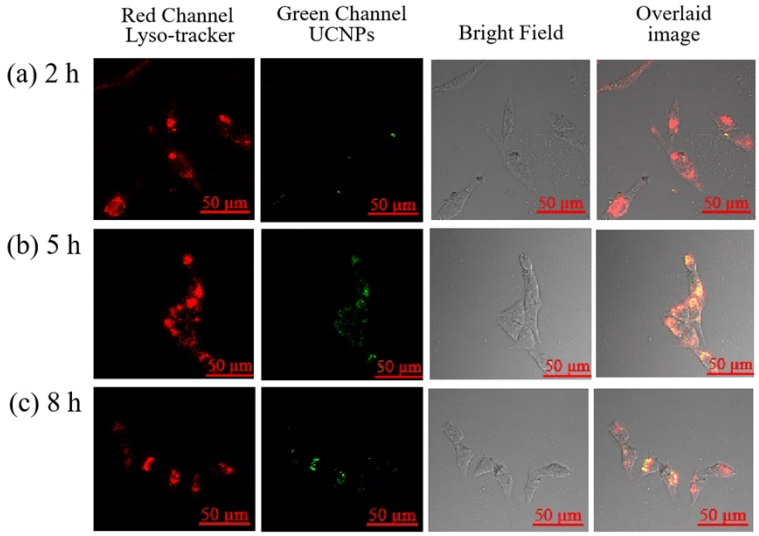

Figure S19: Confocal laser scanning microscopy (CLSM) images of L132 normal cells treated with 80 μg/mL of the prepared nanotheranostic agent for (a) 2 h , (b) 5 h and (c) 8 h. Red channel was used to record the lysosome fluorescence meanwhile green channel was used to record the fluorescence information of the designed nanotheranostic agent.

Besides, the cell uptake and targetability of the nanocarriers without the outer DNA, that is UCNPs@mSiO$_2$/MB@PAH nanoprobe, were investigated. As demonstrated in Figure S20, the designed UCNPs@mSiO$_2$/MB@PAH nanoprobe could be endocyted into L132 normal cells and A549 cancer cells without significant difference in the cell uptake owing to the absence of the surface MUC1 aptamer.

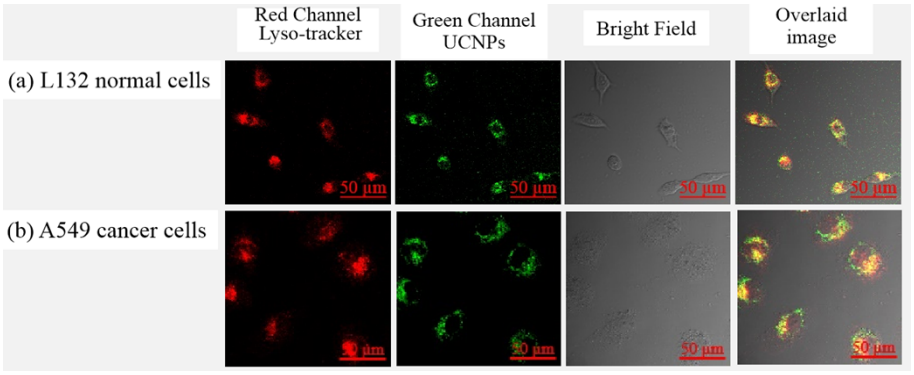

Figure S20: Confocal laser scanning microscopy (CLSM) images of L132 normal cells and A549 cancer cells treated with 80 μg/mL of the UCNPs@mSiO$_2$/MB@PAH nanoprobe for 8 h. The lysosome florescence information was recorded in the red channel with the wavelength range of 575-635 nm under the excitation of 561 nm and the fluorescence information of the designed nanotheranostic agent was recorded in the green channel with wavelength range of 500-570 nm under the excitation of 980 nm laser.

5.4 Intracellular DOX release

A549 cancer cells cultured in the glass coverslips was incubated with the prepared nanotheranostic agent (80 μg/mL) for different time. After removed the excess probes, A549 cancer cells was stained with Lysotracker Red and Hoechst 33342, and then observed the

lysosome and nucleus under the laser confocal scanning microscope. The fluorescence information of DOX molecules, lysosome and nucleus was as followed. Blue channel was collected at 410-460 nm under the excitation of 405 nm to obtain the fluorescence information of nucleus; Green channel was collected at 525-620 nm under the excitation of 488 nm to obtain the fluorescence information of DOX molecules; Red channel was collected at 575-635 nm under the excitation of 561 nm to obtain the fluorescence information of lysosome.

For cytometry, A549 cancer cells were incubated with 80 μg/mL of the prepared nanomaterials for 12 h and then washed with PBS buffer to remove the excess nanoprobe. After that, the treated A549 cancer cells were collected with the trypsin digestion, washed with PBS for twice and injected into flow cytometry to collect the average fluorescence information of released DOX molecules. As shown in Figure S21, A549 cancer cells displayed negligible DOX fluorescence when treated with the control nanoprobe while there was obvious DOX fluorescence due to the triggered release when treated with the prepared UCNPs@mSiO$_2$/MB@PAH@DNA nanoshell/DOX.

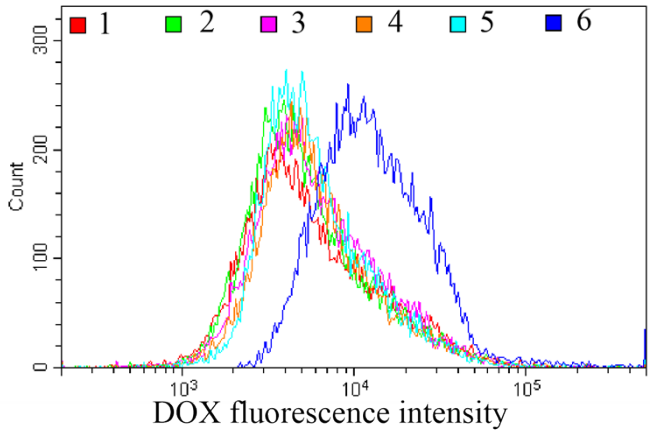

Figure S21: Cytometry analysis of DOX fluorescence intensity of A549 cancer cells with different treatments. 1: without any treatment; 2: irradiated with NIR laser; 3: incubated with 80 μg/mL of the prepared UCNPs@mSiO$_2$@PAH@DNA nanoshell for 12 h; 4: incubated with 80 μg/mL of the prepared UCNPs@mSiO$_2$@MB nanoprobe for 12 h and then irradiated with NIR laser; 5: incubated with 80 μg/mL of the prepared UCNPs@mSiO$_2$@MB@PAH@DNA nanoshell for 12 h; 6: incubated with 80 μg/mL of the prepared UCNPs@mSiO$_2$@MB@PAH@DNA nanoshell/DOX for 12 h.

5.5 In vitro ROSs generation

The *in vitro* ROSs generation was analyzed with the cellular ROSs indicator, 2',7'-dichlorofluorescin diacetate (DCFH-DA) by the laser confocal scanning microscope and the flow cytometry. To *in-situ* observe the production of cellular ROSs, A549 cancer cells were firstly incubated with/without 10 μM oligomycin or 5 mM Ca^{2+} or 500 μM LPA for 30 min, and then incubated with the designed nanotheranostic agent for 12 h, washed with the sterilized

PBS buffer to remove the excess nanomaterials, and irradiated under the 980 nm continuous-wave laser (1.5 w/cm^2, 4 min). Then, the treated A549 cancer cells was stained with diluted DCFH-DA staining solution for 30 min, washed with sterilized PBS buffer for several times and then observed the fluorescence information under the laser scanning confocal microscope. It was reported that DCFH-DA was firstly esterized by relative esterase and then oxidized into DCF by cellular ROSs which showed bright green fluorescence in the emission wavelength from 500 nm to 570 nm under the excitation at 488 nm.

Subsequently, the average fluorescence information of DCF in A549 cancer cells was analyzed with the flow cytomerty. A549 cancer cells were incubated with the prepared nanomaterials and washed with PBS buffer. Then, the treated A549 cancer cells were collected with the trypsin digestion and divided into two parallel subgroups. One group was used as the irradiation group which was irradiated under 980 nm continuous-wave laser while the other group was used as the control group without irradiation. After treatment, both of the two parallel subgroups were resuspended in the diluted DCFH-DA solution for 30 min. Finally, the cell was washed with PBS for twice and injected into the flow cytometry to obtain their fluorescence information.

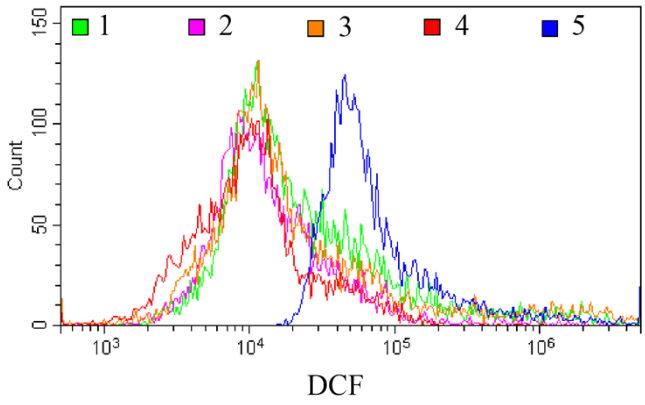

Figure S22: Cytometry analysis of DCF fluorescence intensity of A549 cancer cells when treated with different nanoprobes. 1: A549 cancer cells without any treatment; 2: A549 cancer cells irradiated with NIR laser; 3: A549 cancer cells incubated with 80 μg/mL of the prepared UCNPs@mSiO$_2$@PAH for 12 h; 4: A549 cancer cells incubated with 80 μg/mL of the prepared UCNPs@mSiO$_2$@PAH@DNA nanoshell for 12 h and then irradiated with NIR; 5: A549 cancer cells incubated with 80 μg/mL of the prepared UCNPs@mSiO$_2$@MB@PAH@DNA nanoshell/DOX for 12 h and then irradiated with NIR.

5.6 Cell apoptosis assay in living cells

In this experiment, the cell apoptosis ratio induced by the prepared nanotheranostic agent was evaluated with the commerical apoptosis detection kit by the flow cytometry. Briefly, A549 cancer cells were treated as the above procedure in section 5.5 including incubated with the

prepared nanotheranostic agent or the control nanomaterials, collected with the trypsin digestion and irradiated under 980 nm continuous-wave laser. Then, A549 cancer cells were uniformly dispersed in 1.0 mL of apoptosis staining solution consisting of 195 μL binding buffer, 5 μL Annexin V-APC staining solution and 10 μL 7-AAD staining solution. After 10 min, the stained A549 cancer cells were washed with PBS for several times and then resuspended in PBS for the following flow cytometry analysis. To be mentioned, the necessary fluorescence compensation must be operated according to the manufacturer's instructions.

As shown in the scatter grams (Figure S23), the negative control group including cell without any treatment, cell with only laser irradiation, cell treated with the corresponding nanoprobe UCNPs@mSiO$_2$/PAH@DNA nanoshell, displayed the high cell viability and low cell apoptosis ratio. After treated with the photodynamic nanotheranostic agent, UCNPs@mSiO$_2$/MB@PAH@DNA nanoshell, A549 cancer cells shifted from the high viability to 20.66% of early apoptosis and 26.15% of late apoptosis while A549 cancer cells treated with the chemotherapy carrier, UCNPs@mSiO$_2$@PAH@DNA nanoshell/DOX, around 20.10% of early apoptosis and 26.86% of late apoptosis would be induced. As compared, after incubated with the finally designed nanotheranostic agent UCNPs@mSiO$_2$/MB@PAH@DNA nanoshell/DOX and then irradiated with the laser, A549 cancer cells would be induced around 7.80% of early apoptosis and 54.17% of late apoptosis. Thus, the apoptosis was a major cell death modality in A549 cancer cells when treated with the designed nanotheranostic agent in this experiment.

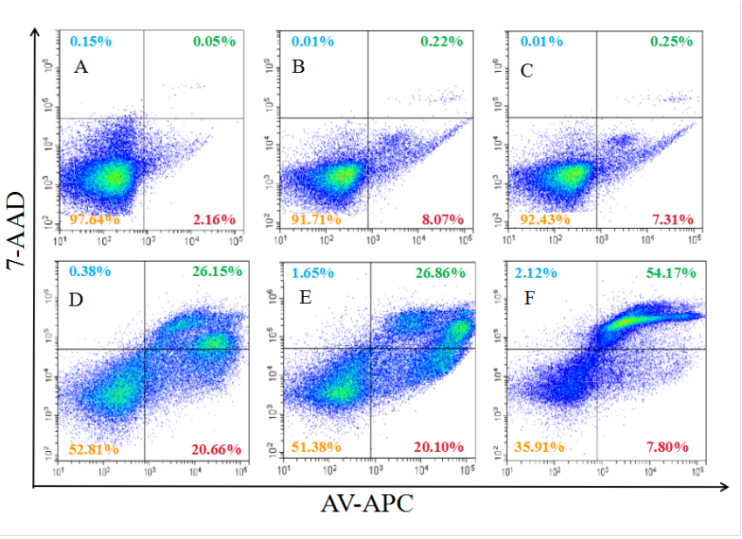

Figure S23: Apoptosis of MCF-7 cancer cells (A) without treatment (B) only irradiated with 980 nm laser (1.5 W/cm^2, 4 min); (C) only incubated with the prepared UCNPs@mSiO$_2$@PAH@DNA nanoshell for 12 h; (D) incubated with the prepared UCNPs@mSiO$_2$/MB@PAH for 12 h and then irradiated with 980 nm laser; (E) incubated with the prepared UCNPs@mSiO$_2$@PAH@DNA nanoshell/DOX for 12 h; (F) incubated

with the prepared UCNPs@mSiO$_2$/MB@PAH@DNA nanoshell/DOX for 12 h and then irradiated with 980 nm laser.

6. Animal experiment

6.1 Obtain the tumor-bearing model

The *in vivo* therapeutic efficacy of the proposed nanotheranostic agent were evaluated with the animal experiment. And the animal care and handing procedures were reviewed and approved by the Animal Care and Use Committee of Linyi University. To obtain the tumor-bearing model, the right leg of purchased Balb/c nude mouse (6 weeks, around 20 g) was injected with around 1×10^6 cancer cells to grow the tumor. The experiment started when the tumor section would grow to the tumor volume of 120-150 mm^3. Tumor-bearing nude mice were randomly into six or groups and each group contained five parallel mouse mode.

6.2 In vivo biodistribution and metabolism of the prepared nanotheranostic agent

The *in vivo* biodistribution and metabolism of the prepared nanotheranostic agent, UCNPs@mSiO$_2$@PAH@DNA nanoshell/DOX, in mice were investigated by using fluorescence bioimaging. As the tumor volume reached to around 300 mm^3, the mice were administered with an intravenous injection of the prepared nanotheranostic agent at the dose of 2.0 mg/mL (50 μL), and then subjected to fluorescence imaging using a IVIS Lumina Series III at different time. As shown in Figure S24a, a strong fluorescence signal in the tumor area and lung was observed after 4 h. Then, the fluorescence intensity of the prepared nanotheranostic agent in mice lung was gradually increased from 4 h to 12 h, and gradually decreased. Meanwhile, the fluorescence intensity of the prepared nanotheranostic agent in mice kidney was increased and reached its maximum at 24 h. After that, the mice kidney displayed obvious decreased fluorescence intensity while the tumor section could maintain the strong intensity at 48 h due to the enhanced permeability and retention effect (EPR). At 48 h post administration, the nude mice were sacrificed to obtain the tumor and normal organs for the further *in vivo* fluorescence imaging. The strongest fluorescence signals were observed at the tumor site and lung compared with other normal organs (Figure S24b). Thus, the results above indicated that the prepared nanotheranostic agent could accumulate in the tumor section via reticuloendothelial systems (RES) absorption and further metabolized in lung, kidney and spleen possibly by the way of feces and urine.[9]

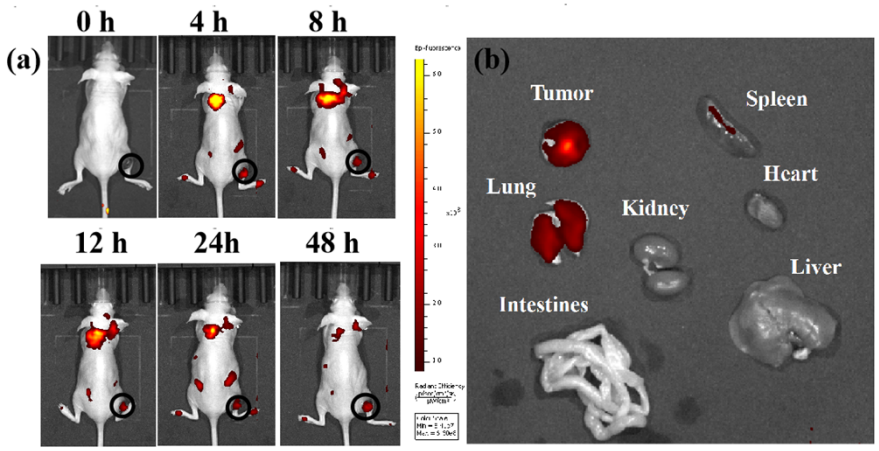

Figure S24: (a) *In vivo* fluorescence imaging and biodistribution of nude mice bearing tumors at different time points after intravenous injection of the prepared nanotheranostic agent (the blank ring pointed out the tumor location in mice); (b) fluorescence imaging of mice main organs after treated with the prepared nanotheranostic agent for 48 h. The florescence information was recorded in the wavelength range of 500-570 nm under the excitation of 980 nm laser.

6.3 In vivo therapeutic efficacy assay

Different treatments was designed and each group contained five parallel mice. The designed treatments were as follows: (A) only injected with PBS; (B) laser irradiation alone; (C) only injected with the control nanomaterial UCNPs@mSiO$_2$@PAH@DNA nanoshell; (D) only injected with the photodynamic nanotheranositc agent, UCNPs@mSiO$_2$/MB@PAH and then irradiated; (E) injected with the chemotherapy agent, UCNPs@mSiO$_2$@PAH@DNA nanoshell/DOX; (F) injected with the final nanotheranostic agent and then irradiated. The experiment operation procedure was as followed. The prepared nanotheranostic agent (50 μL, 2.0 mg/mL) was injected into the tumor section. After overnight, 980 nm laser was used to irradiate the tumor section for 4 min (1.5 W/cm^2, 1 min interval). Then, the tumor volume was calculated every two days based on the equation V=length×width^2/2. Considering its metabolism, the prepared nanotheranostic agent was injected into the tumor section and irradiated with the laser again. After recorded its tumor changes over a period for 13 days, the mouse was sacrificed to obtain the tumor section and main organs which were sliced for the following immuno-staining analysis including hematoxylin and eosin (H&E) staining, TUNEL staining and Caspase-3 staining.

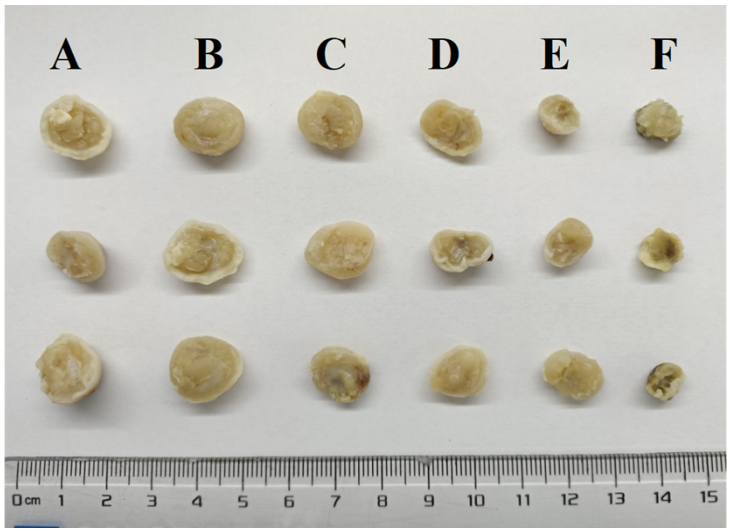

Figure S25: Photographs of the dissected tumor section on the thirteen days with different treatments.

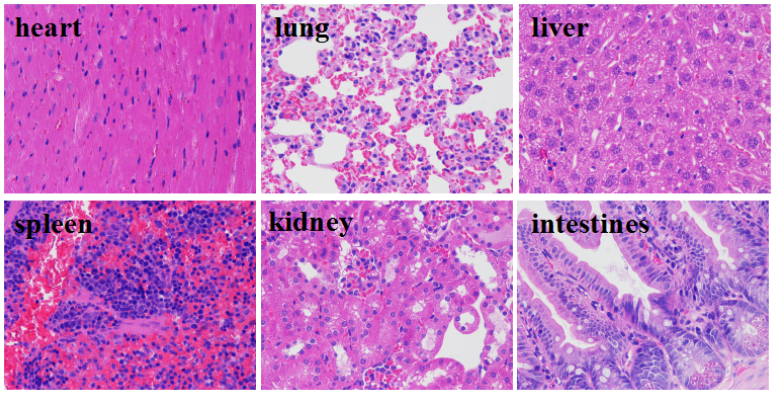

Figure S26: Bio-toxicity investigation of the prepared UCNPs@mSiO$_2$@PAH@DNA nanoshell/DOX nanotheranostic agent to the main organs.

Reference

1. (a) X. Y. Song, Z. H. Yue, T. T. Hong, Z. H. Wang and S. S. Zhang, *Anal. Chem.,* 2019, **91**, 8549; (b) X. Y. Song, Z. H. Yue, J. Y. Zhang, Y. X. L. Jiang, Z. H. Wang and S. S. Zhang, *Chem. Eur. J.,* 2018, **24**, 6458.

2. J. N. Liu, W. B. Bu and J. L. Shi, *Acc. Chem. Res.,* 2015, *48*, 1797.

3. J. N. Liu, W. B. Bu, S. J. Zhang, F. Chen, H. Y. Xing, L. M. Pan, L. P. Zhou, W. J. Peng and J. L. Shi, *Chem. Eur. J.,* 2012, **18**, 2335.

4. (a) V. Muhr, C. Würth, M. Kraft, M. Buchner, A. J. Baeumner, U. Resch-Genger and T. Hirsch, *Anal. Chem.,* 2017, **89**, 4868; (b) L. Mattsson, K. D. Wegner, N. Hildebrandt and T. Soukka, *RSC Adv.,* 2015, **5**, 13270.

5. B. Wu, Z. Q. Cao, Q. Zhang and G. J. Wang, *Sensors and Actuators B: Chemical,* 2018, **255**, 2853.

6. (a) D. C. Wimalachandra, Y. Li, J. L. Liu, S. Shikha, J. Zhang, Y. C. Lim and Y. Zhang, *ACS Appl. Mater. Interfaces,* 2019, **11**, 37513; (b) H. Zhu, J. H. Deng, Y. Y. Yang, Y. F. Li, J. C. Shi, J. K. Zhao, Y. Deng, X. C. Chen and W. Z. Yang, *Colloid Surface B.,* 2019, **180**, 401; (c) Z. G. Teng, S. J. Wang, X. D. Su, G. T.

Chen, Y. Liu, Z. M. Luo, W. Luo, Y. X. Tang, H. X. Ju, D. Y. Zhao and G. M. Lu, *Adv. Mater.,* 2014, **26**, 3741.

7. (a) C. Zhang, W. H. Chen, L. H. Liu, W. X. Qiu, W. Y. Yu and X. Z. Zhang, *Adv. Funct. Mater.,* 2017, **27**, 1700626; (b) Y. Chong, C. Ge, G. Fang, X. Tian, X. Ma, T. Wen, W. G. Wamer, C. Chen, Z. Chai and J. J. Yin, *ACS Nano*, 2016, **10**, 8690.

8. (a) D. Yang, G. X. Yang, Q. Q. Sun, S. L. Gai, F. He, Y. L. Dai, C. N. Zhong and P. P. Yang, *Adv. Healthc. Mater.,* 2018, **7**, 1800042; (b) I. S. Turan, D. Yildiz, A. Turksoy, G. Gunaydin and E. U. Akkaya, *Angew. Chem.,* 2016, **128**, 2925; (c) F. Y. Li, Y. Du, J. N. Liu, H. Sun, J. Wang, R. Q. Li, D. Kim, T. Hyeon and D. S. Ling, *Adv. Mater.,* 2018, **30**, 1802808.

9. L. Q. Peng, X. Mei, J. He, J. K. Xu, W. K. Zhang, R. Z. Liang, M. Wei, D. G. Evans and X. Duan, *Adv. Mater.,* 2018, **30(16)**, 1707389.